Towards Slot Bonding for Adaptive MCS in IEEE 802.15.4e TSCH networks

Glenn Daneels, Carmen Delgado, Steven Latré, Jeroen Famaey
IDLab, University of Antwerp - imec
Antwerp, Belgium
firstname.lastname@uantwerpen.be

***Abstract*—Low-power wireless mesh networks provide connectivity for a wide range of applications in industrial scenarios. For many years, IEEE 802.15.4e Time-Slotted Channel Hopping (TSCH) networks have proven their efficiency in such environments, providing high reliability and low-power operation. TSCH networks run on top of one physical (PHY) layer and are thus limited by the characteristics of the chosen PHY layer in terms of, among others, data rate, reliability and energy efficiency. To tackle these limitations and to improve network performance and flexibility in those challenging industrial environments, this work explores the simultaneous use of multiple PHYs, and more specifically multiple modulation and coding schemes (MCSs), in a TSCH network. Traditionally, TSCH relies on fixed-duration slots, large enough to send a packet of any size given the fixed data rate. In order to avoid wasting airtime when simultaneously using multiple PHYs or MCSs with different data rates, we first introduce the concept of slot bonding. This allows the creation of different-sized bonded slots with a duration adapted to the data rate of each chosen PHY. Afterwards, we formally describe TSCH slot bonding using a Mixed Integer Linear Program (MILP) model. Finally, we use this model to determine the optimal MCS configuration with a short slot frame length that causes network saturation and show the scalability advantage of slot bonding in terms of packet delivery ratio.**

***Index Terms*—Slot bonding, TSCH, wireless mesh networks, IEEE 802.15.4e**

I. Introduction

A wide range of industrial applications benefit from the connectivity provided by low-power wireless mesh networks, which vary from time-critical remote control of machinery to continuous monitoring of industrial valves [1]. The requirements are application-dependant and defined by a trade-off between low delay, high reliability and low-power operation.

Over the years, the IEEE 802.15.4 standard [2] has been the preferred solution to tackle a major part of such challenging applications. The standard defines a variety of physical (PHY) and Medium Access Control (MAC) layers for low-power wireless networks in the sub-GHz and $2.4\,\mathrm{GHz}$ frequency band. The later introduced IEEE 802.15.4e-2012 amendment proposed the Time-Slotted Channel Hopping (TSCH) MAC layer to combat external interference and multi-path propagation effects in challenging wireless environments. In a tightly-synchronized time-slotted schedule, it uses frequency diversity to provide high reliability while maintaining low-power operation. TSCH has been the basis for the IPv6 over the TSCH mode of IEEE 802.15.4e (6TiSCH) standardization group that aims at the adoption of IPv6 in industrial standards [3].

For many years, TSCH as a MAC layer has proven its efficiency in various low-power wireless mesh scenarios. However, traditionally TSCH runs on top of a single PHY layer and is thus limited by the characteristics of the chosen PHY in terms of data rate, transmission range, interference robustness and energy consumption. Being often deployed in challenging wireless environments such as large industrial sites with blocking metal constructions disrupting the wireless connection, the performance of a TSCH network could significantly improve from being able to use multiple PHY layers in its network simultaneously and adapt the PHY of each link to the local conditions and the application's requirements.

In this work, we explore the exploitation of multiple PHY layers offered in IEEE 802.15.4g, and specifically multiple modulation and coding schemes (MCSs) of the Orthogonal Frequency Division Multiplexing (OFDM) PHY layer. Therefore, we first introduce the concept of TSCH *slot bonding* which allows the creation of different-sized bonded slots with a duration adapted to the data rate of each chosen PHY. Slot bonding thus facilitates the use of multiple PHYs (or multiple MCSs) within a single TSCH network in a resource-efficient manner. In contrast, traditional TSCH relies on fixed-duration slots, large enough to send a packet of any size given the fixed data rate, which results in wasted airtime if different MCSs with different data rates are used simultaneously. To the best of our knowledge, we are the first to propose slot bonding in TSCH. Further, we formally describe TSCH slot bonding using a Mixed Integer Linear Program (MILP) formulation that optimizes the network packet delivery ratio while keeping the energy consumption minimized by deciding on the optimal TSCH schedule allocations. We use this MILP formulation during extensive TSCH simulation experiments to show the optimal MCS configuration with a short slot frame length that causes network saturation and prove the scabalability advantage of slot bonding over longer fixed-durations slots in terms of network-wide packet delivery ratio (PDR).

II. Related work

Supporting multiple MCSs is a well-established feature in many standards such as IEEE 802.11 [4] and Long Term Evolution (LTE) Release 8 [5]. In TSCH, to the best of our knowledge, the simultaneous support of multiple PHYs or MCSs in a single network has not yet been investigated. However, recent IEEE 802.15.4(g) research efforts hint to the

promising possibilities and the use of the more robust OFDM and all its different MCSs [6], [7]. At the same time, Muñoz et al. [8] show that, even when applying OFDM at the physical layer, a channel hopping approach at the MAC layer such as TSCH, is still required to have reliable links.

The introduction of TSCH, that applies MAC layer channel hopping to mitigate multi-path fading effects, was a major step towards more reliable low-power wireless mesh networks. Since then, countless TSCH scheduling solutions have been proposed varying from centralized ones, such as TASA [9], to distributed functions, such as Wave [10]. Recently, autonomous functions, such as Orchestra [11], gained popularity as their allocations solely depend on the available routing information and do not need external aid. While these scheduling functions try to find the optimal trade-off between throughput, latency and energy consumption for the given application, their performance still heavily depends on environmental factors, such as external interference and multi-path fading effects. To cope with those effects, channel blacklisting techniques, such as MABO-TSCH [12], that identify bad channels and distribute this knowledge, have also been proposed [13].

While TSCH scheduling functions and blacklisting techniques offer valid solutions to deal with various link conditions, they are still limited by the employed PHY. That is why we believe that by *additionally* offering PHY layer flexibility, the reliability of a TSCH network and its performance in general would drastically improve.

III. TSCH Slot Bonding

Each PHY layer in the IEEE 802.15.4g standard has its own set of characteristics in terms of computational complexity, energy consumption, range, robustness and data rate. We propose the use of multiple PHYs in TSCH, using *slot bonding*. In this section, we reiterate the basic concept of the TSCH schedule matrix, apply slot bonding and explain its advantages.

A. TSCH Schedule Matrix

In a TSCH network, all the nodes are time-synchronized. Each node maintains a matrix-formatted schedule in which time is split up in fixed-duration time slots. A time slot is long enough to send a maximum packet of 127 bytes and receive an acknowledgement (ACK) and the optimal duration thus depends on the data rate of the chosen PHY. Time slots are grouped in slot frames which are repeated over time, and whose size is application-dependent. The Absolute Sequence Number (ASN) defines the absolute time in TSCH, which starts with 0 at the first ever time slot and increments with 1 in every time slot that follows. A time slot in a slot frame is denoted by its time slot offset which, together with a channel offset, defines one element in the schedule, a *schedule cell*. To do channel hopping, the channel offset is used together with the ASN to pseudo-randomly select the frequency channel at which the packet in that cell will be transmitted.

The TSCH schedule instructs a node what to do at each slot in a slot frame: sleep, transmit or listen. A scheduled cell between two nodes is *dedicated* by default, i.e., it is reserved only for those two nodes. A cell can also be marked as *shared*, which means that multiple nodes can send at the same time and a back-off timer is applied to avoid contention. A scheduled cell can be marked as a *transmit* cell, in which a node transmits a queued packet, or as a *receive* cell in which the node listens for a possible incoming packet.

B. Multiple PHYs

As mentioned above, the IEEE 802.15.4g standard defines a variety of PHY layers, for example, OFDM, that was created to combat multi-path fading, as well as Frequency Shift Keying (FSK) and Offset-Quadrature Phase Shift Keying (O-QPSK) [2], [7]. We propose to exploit the characteristics of the different available PHYs (or MCSs) in the IEEE 802.15.4 standard for different links in a TSCH network. This will allow us to tailor the performance of each link to the local environmental conditions and the application's requirements.

Using different PHYs in the same network has an impact on both the time slot and channel management in a TSCH schedule. As different PHYs are computationally different and have different data rates, their processing and transmission time directly impacts the optimal TSCH slot length, which should encompass the time it takes to send a data packet and receive an ACK. At the same time, different PHYs can require different bandwidths, which influence both the total number of available frequency channels in a TSCH schedule and the effective number of channels a transmission would need to bond together to send the data. For both the time slot and channel management when supporting multiple PHYs, we propose the concepts of *slot* and *channel bonding* respectively, which can be applied combined or used separately. The former bonds multiple *regular* time slots to a bonded slot which has the necessary length to transmit or receive data given the selected PHY's data rata and computational time. The latter bonds multiple available frequency channels to allocate the necessary bandwidth to accommodate the chosen PHY. In contrast to a more greedy approach of configuring the TSCH schedule with cells that are long enough in time and occupy a bandwidth wide enough to be compatible with all supported PHYs at once, the proposed slot and channel bonding technique tailors each bonded slot to the requirements of the specific PHY. It thus has the advantage of limiting the waste of both airtime and bandwidth resources.

Figure 1 shows an example of a TSCH schedule that applies both slot and channel bonding. The physical layer *PHY1* applied for the link from node X to the root requires a $30\,\mathrm{ms}$ bonded time slot and the bonding of two $200\,\mathrm{kHz}$ frequency channels to a $400\,\mathrm{kHz}$ bandwidth. *PHY2* used for the link from node Y to the root requires the bonding of two $10\mathrm{ms}$ time slots to a $20\,\mathrm{ms}$ time slot in order to be able to transmit a packet and receive an ACK. The minimal shared cell to bootstrap the network, indicated by the orange bonded slot in the figure, is configured with the same PHY1 physical layer.

In this first work towards supporting multiple PHYs, we focus solely on slot bonding and make use of the flexibility of OFDM as it provides various data rates for a single bandwidth.

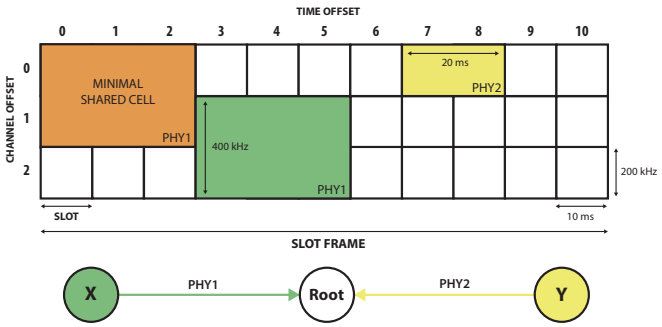

Fig. 1. A TSCH schedule with regular slots of 10 ms length and 200 kHz bandwidth. For accommodating PHY1 on the link from node X to the root both slot and channel bonding are applied while for PHY2 on the link from node Y to the root only slot bonding is considered.

TABLE I
MCSs OF OFDM OPTION 4 WHICH ALL REQUIRE 200 kHz BANDWIDTH.

Mode	Modulation, Code rate, Freq. rep.	Datarate (kbps)	Radio on (ms)	# Regular slots per bonded slot	
				10 ms	30 ms
MCS2	O-QPSK, 1/2, 2x	50	26.56	3	1
MCS3	O-QPSK, 1/2, 0	100	14.24	2	1
MCS4	O-QPSK, 3/4, 0	150	10.13	2	1
MCS5	16-QAM 1/2, 0	200	8.08	2	1
MCS6	16-QAM 3/4, 0	300	6.03	1	1

In our future work, we will extend this work with channel bonding. The OFDM PHY layer that was introduced in the IEEE 802.15.4g-2012 amendment offers 31 PHY variations, which are subdivided in 4 different *options* that determine how many sub-carriers are grouped together in order to form an OFDM channel [7]. Each option has its own specific bandwidth requirement and also a set of different MCS values that determine how each sub-carrier is modulated (and whether frequency repetition and Forward Error Correction (FEC) is applied). Each MCS value has its own computational complexity and a different data rate which results in a different optimal time slot length. These different lengths translate to bonded slots with different numbers of regular slots, as shown in Table I for regular slots of lengths 10 ms and 30 ms. To calculate the necessary number of regular slots per bonded slot, we take into account the radio on time for a specific MCS and assume 3 ms of CPU processing time per bonded slot, in line with the values reported in [14] using a subGHz radio. The radio on time for each MCS was calculated for a 127 bytes data packet and a 27 byte ACK (i.e., the default size in TSCH to determine the slot duration), using the data rate of the respective MCS and also including the duration for sending the OFDM Synchronization Header (SHR) and PHY Header (PHR) in the lowest MCS of the chosen OFDM option, i.e., MCS2 of option 4 in this case [7].

C. Slot Bonding

Slot bonding encompasses the aggregation of at least two regular slots in the same frequency channel to one bonded slot to support transmissions at a lower data rate. In this section we detail how several aspects of a normal TSCH network process are affected by applying slot bonding.

1) Preparing the TSCH layer: When applying slot bonding, the general concepts of the TSCH schedule as described in Section III-A do not change. However, slot bonding introduces the additional concept of a *bonded slot*. A bonded slot performs the same actions as a regular slot, but the timings of the different actions (e.g., preparing, transmitting, receiving a packet) depend on the underlying PHY layer and (can) occupy more time than one regular slot. These state timings used in all possible PHY variations should be known beforehand to all nodes to maintain the strict synchronization of TSCH schedule.

2) Bootstrapping the network: The Minimal 6TiSCH Configuration defines a *minimal cell* to provide minimal connectivity between the nodes in the network [15]. A distributed scheduling function can use this cell to bootstrap the network. When supporting multiple PHYs, the minimal cell could be configured to use the PHY that has the best robustness and range features to allow all nodes to bootstrap, meaning that the minimal cell will likely be a bonded cell.

3) Negotiating a bonded slot: The process of allocating a bonded slot is very similar to the traditional 6top Protocol (6P) transaction to allocate a TSCH cell [16]. In addition to the conventional negotiation between two nodes, the nodes also agree on the underlying PHY layer which can be specified in the reserved bits in the *CellOptions* bitmap when adding the bonded slot [16]. When a node wants to change the PHY of a particular bonded slot, it can issue a 6P *RELOCATE* request to its neighbor that does not relocate the cell but mentions another PHY index in the *CellOptions* bitmap. The specific problem of dynamically adapting the PHY to the requirements of the application is independent of the concept of slot bonding and is thus out of scope of this paper and reserved for future work.

IV. TSCH Slot Bonding Model

This section formally describes the IEEE 802.15.4e TSCH slot bonding scheduling problem in which the PDR of the network is maximized while the energy consumption is minimized by limiting the radio on time. We formulate the underlying optimization problem as a MILP that uses, among others, the possible MCSs and network topology as input and decides on the optimal schedule allocations and MCSs for each link. The MILP assumes an already formed tree-based topology, meaning that every node is already appointed a parent node, e.g., based on a routing protocol such as IPv6 Routing Protocol for Low-Power and Lossy Networks (RPL). All data is assumed to be sent to the root, with 1 generated packet per slot frame per node. The remainder of this section describes the different aspects of the MILP formulation.

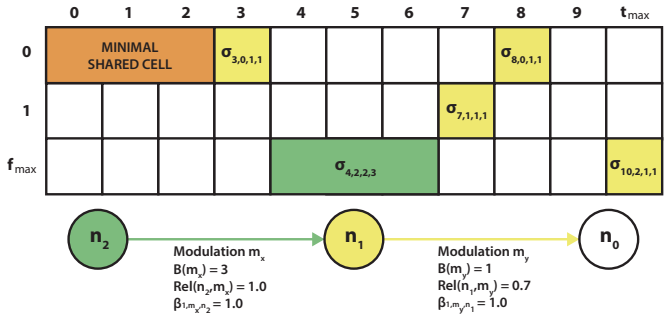

Fig. 2. Illustration of the ILP input and decision variables in a three node topology, with β_{1,m_x,n_2} and β_{2,m_y,n_1} equaling 1 for the links from n_2 to n_1 and from n_1 to n_0 respectively.

A. Input variables

The network consists of a set of nodes $N = \{n_0, n_1, ..., n_{max}\}$, of which node n_0 is the root, i.e., the sink node. N_0 represents the set of nodes without the root. Each node $n \in N_0$ has a parent node $p_n \in N$ and a set of children $C_n \subset N_0$. The set of slots in a slot frame are denoted by $T = \{t_0, t_1, ..., t_{max}\}$ and the set of channel offsets at which a node can transmit are represented by $F = \{f_0, f_1, ..., f_{max}\}$.

The number of bonded slots that a node allocates in one slot frame to successfully transmit one particular packet, i.e., the transmission opportunities per packet, is represented by $r \in R$, with $R = \{0, 1, ..., R_{max}\}$, where R_{max} is configurable.

The reliability of the link from $n \in N_0$ to its parent $p_n \in N$, where $m \in M$, with $M = \{m_0, m_1, ..., m_{max}\}$ is the MCS for the underlying PHY, is defined by $L(n, m) \in [0, 1]$. The number of consecutive regular slots in one bonded slot is represented by $s \in S$, with $S = \{B(m_0), B(m_1), ..., B(m_{max})\}$, where the auxiliary symbol $B(m) \in \mathbb{N}_{>0}$ returns the exact number of regular time slots that need to be bonded to transmit a 127 byte packet and receiving an ACK given MCS $m \in M$.

The number of milliseconds the radio is on when transmitting a packet of 127 bytes and receiving an ACK, when using MCS $m \in M$, is represented by $O(m) \in \mathbb{R}_{>0}$. We assume that each node generates 1 packet per slot frame, but our model can be trivially extended to multiple transmissions per node.

B. Decision variables

There are two decision variables $\sigma_{t,f,n,s}$ and $\beta_{r,m,n}$ in the MILP which together represent the specific resource allocations a node should make in its TSCH schedule:

- $\sigma_{t,f,n,s}$ is a binary variable that is 1 when node $n \in N_0$ transmits in a bonded slot that consists of s consecutive slots allocated at time offsets $\{t, t+1, \ldots, t+(s-1)\} \subset T$ and channel offset $f \in F$ in the TSCH schedule matrix to its parent $p_n \in N$, else it is 0.
- $\beta_{r,m,n}$ is a binary variable that is 1 when node $n \in N_0$ uses MCS $m \in M$ and allows $r \in R$ transmission opportunities per packet in the slot frame to its parent $p_n \in N$.

Figure 2 illustrates the meaning of the decision variables $\sigma_{t,f,n,s}$ and $\beta_{r,m,n}$.

C. Constraints

In the following, the constraints of the MILP are presented.

A node $n \in N_0$ can only use one MCS m and a specific number of transmission opportunities r for all its available packets to its parent:

$$\forall n \in N_0 : \sum_{m \in M} \sum_{r \in R} \beta_{r,m,n} = 1 \quad (1)$$

A transmission of node $n \in N_0$ can not overlap with any other transmission of the same node, nor with any of the transmissions of its children, as a node can only perform one action during each slot:

$$\forall n \in N_0, t \in T : \sum_{f \in F} \sum_{t' \in [0,t]} \sum_{s \in [t-t'+1, (t_{max}+1)-t']} (\sigma_{t',f,n,s} + \sum_{j \in C_n} \sigma_{t',f,j,s}) \leq 1 \quad (2)$$

The transmissions of the children of the root can not be in the same slot, as the root can only listen to one child at once:

$$\forall t \in T : \sum_{f \in F} \sum_{t' \in [0,t]} \sum_{s \in [t-t'+1, (t_{max}+1)-t']} \sum_{j \in C_{root}} \sigma_{t',f,j,s} \leq 1 \quad (3)$$

A bonded slot transmission $\sigma_{t,f,n,s}$ consisting of s consecutive slots should not exceed the slot frame length:

$$\forall n \in N_0, t \in T, f \in F, s \in S : (t + s - 1) \cdot \sigma_{t,f,n,s} \leq t_{max} \quad (4)$$

A node n that uses MCS m to its parent p_n and allows r transmission opportunities per packet, should allocate exactly $S(m)$ consecutive slots for a transmission:

$$\forall n \in N_0, t \in T, f \in F, m \in M, r \in R, s \neq B(m) : \beta_{r,m,n} \cdot \sigma_{t,f,n,s} = 0 \quad (5)$$

The auxiliary integer variable d_n represents the upper bound to the number of packets that a node tries to transmit to its parent and is defined by the total number of transmissions divided by the r transmission opportunities the node allocates for a single packet:

$$\forall n \in N_0 : d_n = \sum_{m \in M} \sum_{r \in R} \frac{\sum_{t \in T} \sum_{f \in F} \sum_{s \in S} \sigma_{t,f,n,s}}{r} \cdot \beta_{r,m,n} \quad (6)$$

The auxiliary continuous variable a_n represents the number of packets that successfully arrive from node n to its parent p_n. Therefore, the upper bound to the number of packets a node tries to transmit has to be smaller or equal to the sum of the packet generated at the node and the (ceiled) number of packets that successfully arrived from each child to node n:

$$\forall n \in N_0 : d_n \leq 1 + \lceil \sum_{j \in C_n} a_j \rceil \quad (7)$$

We represent the link PDR for the transmission of a packet from node n to its parent p_n over a link with reliability

$L(n,m)$ using MCS m, while having r transmission opportunities for that packet by the auxiliary symbol $LPDR(n,m,r)$:

$$LPDR(n,m,r) = (-1)^{(r+1)} \cdot L(n,m)^r + \left[\sum_{i=1}^{r-1}(-1)^{(i+1)} \cdot L(n,m)^i \left[\binom{r-1}{r-i} + \binom{r-1}{i}\right]\right] \quad (8)$$

To maximize the PDR of the network, we want to maximize the number of successfully arrived packets at the root. To do so, we limit a_n to be the minimum of constraints 9 and 10. Consequently, when the MILP tries to maximize all packets that arrive at the root, it will have to maximize a_n of all nodes.

a_n should be less than or equal to the number of packets available at node n, i.e., the one packet generated at node n, and the arrived packets from the children of n, multiplied with the PDR from n to its parent:

$$\forall n \in N_0 : a_n \leq (1 + \sum_{j \in C_n} a_j) \cdot \sum_{m \in M} \sum_{r \in R} \beta_{r,m,n} \cdot LPDR(n,m,r) \quad (9)$$

a_n should also be less than or equal to d_n, multiplied by the PDR of n to its parent p_n:

$$\forall n \in N_0 : a_n \leq \delta_n \cdot \sum_{m \in M} \sum_{r \in R} \beta_{r,m,n} \cdot LPDR(n,m,r) \quad (10)$$

D. Objective function

The objective function aims at maximizing the PDR of the network while minimizing the energy consumption by limiting the time when the radio is on. Therefore we define the total time all radios in the network are active during a slot frame as follows:

$$O_{network} = \sum_{n \in N_0} (\sum_{t \in T} \sum_{f \in F} \sum_{s \in S} \sigma_{t,f,n,s} \cdot \sum_{m \in M} \sum_{r \in R} \beta_{r,m,n} \cdot O(m)) \quad (11)$$

Equation 12 maximizes the number of delivered packets at the root while minimizing the total active radio time. The divisions are added to normalize both objectives to be between 0 and 1. The length of one regular time slot in the TSCH schedule is represented by the constant l and the weight ω can be used to configure the relative importance of both objectives:

$$max(\omega \frac{\sum_{j \in C_{root}} a_j}{|N_0|} - (1-\omega)\frac{O_{network}}{|T| \cdot l \cdot |N_0|}) \quad (12)$$

V. Evaluation

In this section, we evaluate the proposed TSCH slot bonding technique. First, we discuss our simulation configuration. Afterwards, we investigate the scalability and MCS configuation of the slot bonding approach.

A. Experiment Methodology & Setup

To conduct our experiments, we followed a three-step process: first, the network topologies were generated by the 6TiSCH simulator [17], then those topologies were fed to the Gurobi solver[1] that solved the MILP defined in Section IV. Finally, the MILP solution was used as a centralized schedule to make static schedule allocations in the TSCH experiments using the 6TiSCH simulator. The changes to the 6TiSCH simulator[2] and the MILP implementation[3] are publicly available. The number of slots per bonded slot are configured as shown in Table I. Each experiment result is averaged over at least 10 iterations. The error bars in the figures represent the standard error over these iterations.

1) 6TiSCH Simulator: We extended the simulator with a sub-GHz outdoor propagation model based on the 3rd Generation Partnership Project (3GPP) spatial channel model [18] and use 3 200 kHz channels in the 868 - 868.6 MHz band. The simulator supports different MCSs by approximating the bit error rates (BERs) for the 5 MCSs in option 4 of the OFDM PHY which all require a 200 kHz bandwidth per channel, as shown in Table I, based on [19]. The energy consumption was modeled using [20] with the current consumption values of the Atmel AT86RF215 transceiver[4] which is fully compliant with the IEEE 802.15.4g-2015 standard and thus supports OFDM.

The topologies were created by randomly placing nodes until a node had reliable links (i.e., a PDR of at least 65% for MCS2) to all the other nodes, resulting in a fully-meshed topology. The node chose a random parent from all the nodes it had reliable links to. In our experiments, only the PHY and MAC layer were enabled and all other stack layers were disabled. The interference model was disabled as this was not taking into account in the MILP, which is left for future work.

2) Gurobi MILP Solver: The proposed MILP was solved with the Gurobi solver. We configured the MILP input variable $O(m)$ with the values shown in column *Radio on* in Table I, for each possible MCS m. The maximum number of allowed transmission opportunities per packet, denoted by R_{max}, is set to 4 as advised by the 6TiSCH Minimal Configuration [15]. Due to the high computational time required to solve the MILP, we only consider 8 nodes per network and allow the Gurobi MILP solver to terminate when the gap between the lower and upper objective bound is less than 1 %.

B. Results

In this section, we first validate the effectiveness of the MILP. Next, we show the effect of the ω parameter. Finally, we show the scalability of slot bonding and have a closer look at the MCS configurations as scheduled by the MILP.

1) MILP validation: To validate the MILP formulation, defined in Section IV, which provides the schedule allocations for the TSCH simulations, we compare the PDR values

[1] https://www.gurobi.com/

[2] https://github.com/imec-idlab/6tisch-adaptive-mcs

[3] https://github.com/imec-idlab/milp-adaptive-mcs

[4] http://ww1.microchip.com/downloads/en/devicedoc/atmel-42415-wireless-at86rf215_datasheet.pdf

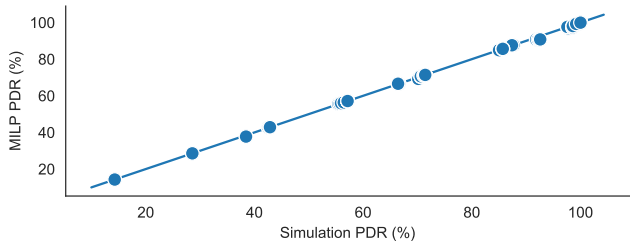

Fig. 3. MILP and simulation PDR results for all experiment iterations for the 10 ms bonded slots and 30 ms slots experiments with a 150 ms slot frame length and 8 node topology.

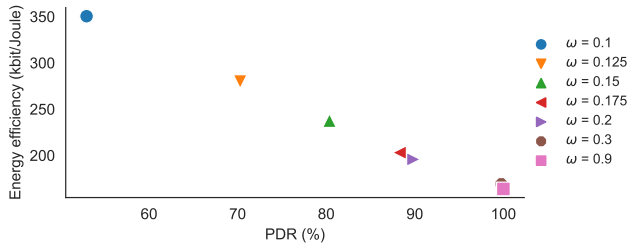

Fig. 4. PDR and energy efficiency comparison for 10 ms bonded slots, 210 ms slot frame length in a 8 node topology.

as calculated in the objective function by the MILP (see Equation 12) with the PDR results of the TSCH simulation (that used the MILP schedule allocations as input). Figure 3 plots the MILP and simulation PDR values against one another for all iterations for the 10 ms bonded slots and 30 ms slots experiments with a 150 ms slot frame length. For all iterations, both values are nearly identical with an overall root mean squared error (RSME) of only 0.3, validating the MILP model to be accurate in terms of calculated PDR.

2) The ω parameter: The weight ω of the objective function of the MILP configures the trade-off of the TSCH scheduler between giving priority to network PDR and being energy efficient. To see its effect, Figure 4 shows the results for 10 ms bonded slots within a network with 210 ms slot frames. As expected, lower ω values decrease the PDR as the MILP will reduce the radio on time of all nodes in the network as defined in Equation 11, meaning it will allocate less cells to optimize energy consumption. Consequently, more packets are dropped because the nodes were unable to transmit them. For example, for $\omega = 0.1$ the PDR got reduced to 53 %, mainly due to the fact that the remaining packets were dropped because there were no available cells (or the transmit queue was already full), while the PDR for $\omega = 0.9$ is 100 %. Meanwhile, because the MILP does not allocate more cells to achieve a high PDR for $\omega = 0.1$, the energy efficiency of $\omega = 0.9$ is less than half that of $\omega = 0.1$, because the former allocates extra cells which increases its energy consumption and PDR. The results also show that for ω ranging from 0.3 to 0.9, the PDR and energy efficiency values do not change significantly.

3) Scalability: To show the effect of slot bonding on scalability, we compare the resource-efficient slot bonding technique with the static approach without slot bonding where a time slot should have a length long enough to accommodate all possible MCSs (and thus valuable slot frame time is wasted for transmissions using MCSs with fast data rates that do not require the maximum slot length). We compare TSCH schedules that contain 10 ms bonded slots to schedules with 30 ms regular slots. Table I shows the number of slots needed for each supported MCS. The 30 ms slots are long enough to support all MCSs and thus no slot bonding is required. We compare both techniques for slot frame lengths of 150 ms, 210 ms and 300 ms, meaning that there are 15, 21 and 30 slots for the slot frame with 10 ms bonded slots and 5, 7 and 10 regular slots for the slot frame with 30 ms slots respectively. The average hop count to the root is 1.9. The ω parameter is set to 0.9 so it optimizes the PDR while taking into account energy efficiency, i.e., setting $\omega = 1$ configures the MILP to drop all energy concerns and allocate as many slots as possible.

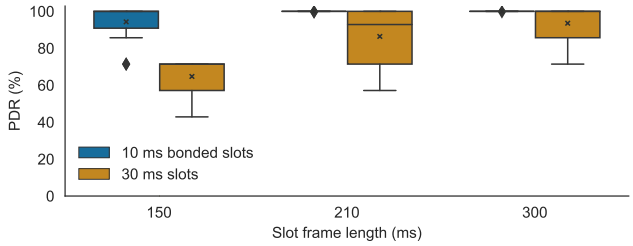

Fig. 5. PDR comparison for 10 ms bonded slots and 30 ms slots, for different slot frame lengths and $\omega = 0.9$. The mean values are denoted with a cross.

Figure 5 shows that the slot bonding technique outperforms the static approach for different slot frame lengths. The average PDR difference between both techniques is 29.6 %, 13.6 % and 6.4 % for the 150 ms, 210 ms and 300 ms respectively. When looking at the energy efficiency, we see that the 30 ms static approach is more energy efficient (with respectively 53.4 %, 14.8 % and 6.2 % for the 150 ms, 210 ms and 300 ms lengths). In all experiments, virtually all packets that did not reach the root were dropped because there were no slots allocated to send the packets, which explains the decreased PDR of the static approach and its increased energy efficiency. Consequently, for both techniques the PDR increases as the length of the slot frame increases and the contention decreases. For each extra slot that the 30 ms static approach wants to allocate, the complete slot length needs to be allocated, i.e., 30 ms. In contrast, the slot bonding technique is more efficient and can choose to allocate an extra slot with an MCS that requires less time (a bonded slot of 10 ms or 20 ms) which could be just short enough and have enough reliability to serve an extra node in the network. These results confirm the scalability advantage of the slot bonding approach over the static approach with fixed 30 ms slot lengths.

4) MCS configuration: To understand how the MILP optimizes PDR for both approaches, we compare the average number of times an MCS is chosen for different ω in the scenario with a short slot frame length that causes network saturation, i.e., 150 ms. The average hop count of this experiment is 1.8. Figure 6 shows the results. The MCSs chosen for the links from all nodes to their parents are plotted, except for the MCSs of the nodes for which there were no allocations to its parent. For all experiments, the average reliability per link from a node to its parent was 0.99 %.

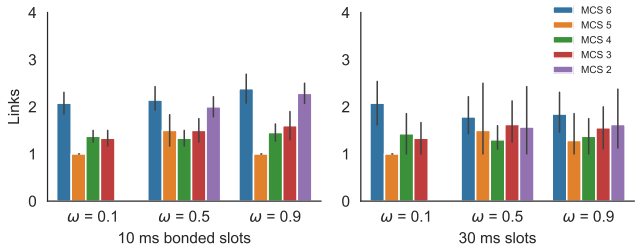

Fig. 6. MCSs for the links from a node to its parent, for a 150 ms slot frame length in a 8 node topology. The MCSs of the nodes for which there were no allocations to its parent are excluded.

For both results where $\omega = 0.1$, it is clear that the MILP saves more energy by not picking the MCS with the slowest data rate (i.e., MCS2) and gives priority to the faster MCSs. When increasing ω to 0.9 and thus focusing more on PDR, both approaches additionally depend on MCS2 with the data rate of 50 kbps. In order to do so, the 30 ms approach had to slightly decrease its MCS6 allocations (i.e., from 2.1 to 1.9), while the slot bonding results actually still increased the average number of MCS6 allocations (i.e., from 2.1 to 2.4). This is explained by the fact that the slot bonding approach is more resource-efficient compared to the 30 ms static approach. This is confirmed by observing the average number of links for which the MILP actually allocated slots (with a maximum of 7 as there are 8 nodes): the slot bonding approach has on average 6.7 links for which the MILP allocated slots, while for the 30 ms slots there are only 4.7 links on average.

VI. Conclusion

This work explored the simultaneous use of multiple PHYs in a IEEE 802.15.4e TSCH network by introducing the concepts of slot and channel bonding. More specifically we focused on slot bonding to support multiple MCSs within the IEEE 802.15.4g OFDM PHY. We formally describe slot bonding in a MILP and use it as a scheduler to make optimal allocations in our TSCH simulations. The simulations show the optimal MCS configuration for the slot bonding approach with a short slot frame length that causes network saturation. Additionally, the results confirm the scalability advantage of the slot bonding approach, in terms of PDR, as it can bond multiple regular slots together in a bonded slot without over-allocating the slot time it needs and thus avoid wasting energy.

Acknowledgment

Part of this research was funded by the Flemish FWO SBO S004017N IDEAL-IoT (Intelligent DEnse And Longe range IoT networks) project, and by the imec ICON project IoS.

References

[1] M. Raza, N. Aslam, H. Le-Minh, S. Hussain, Y. Cao, and N. M. Khan, "A Critical Analysis of Research Potential, Challenges, and Future Directives in Industrial Wireless Sensor Networks," *IEEE Communications Surveys & Tutorials*, vol. 20, no. 1, pp. 39–95, 2017.

[2] *IEEE Standard for Telecommunications and Information Exchange Between Systems - LAN/MAN Specific Requirements - Part 15: Wireless Medium Access Control (MAC) and Physical Layer (PHY) Specifications for Low Rate Wireless Personal Area Networks (WPAN)*, IEEE Std. 802.15.4, 2003.

[3] P. Thubert, "An Architecture for IPv6 over the TSCH mode of IEEE 802.15.4," Internet Engineering Task Force, Internet-Draft draft-ietf-6tisch-architecture-26, Aug. 2019, work in Progress. [Online]. Available: https://datatracker.ietf.org/doc/html/draft-ietf-6tisch-architecture-26

[4] IEEE Computer Society, "IEEE Standard for Information technology–Telecommunications and information exchange between systems Local and metropolitan area networks–Specific requirements - Part 11: Wireless LAN Medium Access Control (MAC) and Physical Layer (PHY) Specifications," *IEEE Std 802.11-2016 (Revision of IEEE Std 802.11-2012)*, vol. 2016, pp. 1–3534, 2016.

[5] 3GPP, "Technical Specification Group Radio Access Network, Study on New Radio Access Technology, Radio Access Architecture and Interfaces (Release 14), 3GPP TR 38.801 V1.0.0," Tech. Rep., December 2016.

[6] J. Muñoz, E. Riou, X. Vilajosana, P. Muhlethaler, and T. Watteyne, "Overview of IEEE802.15.4g OFDM and its Applicability to Smart Building Applications," in *2018 Wireless Days (WD)*. IEEE, 2018, pp. 123–130.

[7] P. Tuset-Peiró, F. Vázquez-Gallego, J. Muñoz, T. Watteyne, J. Alonso-Zarate, and X. Vilajosana, "Experimental Interference Robustness Evaluation of IEEE 802.15. 4-2015 OQPSK-DSSS and SUN-OFDM Physical Layers," *arXiv preprint arXiv:1905.11102*, 2019.

[8] J. Muñoz, P. Muhlethaler, X. Vilajosana, and T. Watteyne, "Why Channel Hopping Makes Sense, even with IEEE 802.15.4 OFDM at 2.4 GHz," in *2018 Global Internet of Things Summit (GIoTS)*. IEEE, 2018, pp. 1–7.

[9] M. R. Palattella, N. Accettura, L. A. Grieco, G. Boggia, M. Dohler, and T. Engel, "On Optimal Scheduling in Duty-cycled Industrial IoT Applications using IEEE802.15.4e TSCH," *IEEE Sensors Journal*, vol. 13, no. 10, pp. 3655–3666, 2013.

[10] R. Soua, P. Minet, and E. Livolant, "Wave: a Distributed Scheduling Algorithm for Convergecast in IEEE 802.15.4e TSCH Networks," *Transactions on Emerging Telecommunications Technologies*, vol. 27, no. 4, pp. 557–575, 2016.

[11] S. Duquennoy, B. Al Nahas, O. Landsiedel, and T. Watteyne, "Orchestra: Robust Mesh Networks through Autonomously Scheduled TSCH," in *Proceedings of the 13th ACM conference on embedded networked sensor systems*. ACM, 2015, pp. 337–350.

[12] P. H. Gomes, T. Watteyne, and B. Krishnamachari, "MABO-TSCH: Multihop and Blacklist-based Optimized Time Synchronized Channel Hopping," *Transactions on Emerging Telecommunications Technologies*, vol. 29, no. 7, p. e3223, 2018.

[13] V. Kotsiou, G. Z. Papadopoulos, P. Chatzimisios, and F. Tholeyre, "Is Local Blacklisting Relevant in Slow Channel Hopping Low-Power Wireless Networks?" in *2017 IEEE International Conference on Communications (ICC)*. IEEE, 2017, pp. 1–6.

[14] G. Daneels, E. Municio, K. Spaey, G. Vandewiele, A. Dejonghe, F. Ongenae, S. Latré, and J. Famaey, "Real-time data dissemination and analytics platform for challenging iot environments," in *2017 Global Information Infrastructure and Networking Symposium (GIIS)*. IEEE, 2017, pp. 23–30.

[15] X. Vilajosana, K. Pister, and T. Watteyne, "Minimal IPv6 over the TSCH Mode of IEEE 802.15.4e (6TiSCH) Configuration," RFC 8180, May 2017. [Online]. Available: https://rfc-editor.org/rfc/rfc8180.txt

[16] Q. Wang, X. Vilajosana, and T. Watteyne, "6TiSCH Operation Sublayer (6top) Protocol (6P)," RFC 8480, Nov. 2018. [Online]. Available: https://rfc-editor.org/rfc/rfc8480.txt

[17] E. Municio, G. Daneels, M. Vučinić, S. Latré, J. Famaey, Y. Tanaka, K. Brun, K. Muraoka, X. Vilajosana, and T. Watteyne, "Simulating 6TiSCH Networks," *Transactions on Emerging Telecommunications Technologies*, vol. 30, no. 3, p. e3494, 2019.

[18] B. Bellekens, L. Tian, P. Boer, M. Weyn, and J. Famaey, "Outdoor IEEE 802.11ah Range Characterization using Validated Propagation Models," in *GLOBECOM 2017-2017 IEEE Global Communications Conference*. IEEE, 2017, pp. 1–6.

[19] G. Pei and T. R. Henderson, "Validation of OFDM Error Rate Model in ns-3," *Boeing Research Technology*, pp. 1–15, 2010.

[20] G. Daneels, E. Municio, B. Van de Velde, G. Ergeerts, M. Weyn, S. Latré, and J. Famaey, "Accurate Energy Consumption Modeling of IEEE 802.15.4e TSCH Using Dual-Band OpenMote Hardware," *Sensors*, vol. 18, no. 2, p. 437, 2018.